J Solid State Electrochem (2006) 10: 439–446
DOI 10.1007/s10008-005-0011-0

ORIGINAL PAPER

Sheela Berchmans · R. G. Nirmal · G. Prabaharan
A. K. Mishra · V. Yegnaraman

Solution phase electron transfer versus bridge mediated electron transfer across carboxylic acid terminated thiols

Received: 27 March 2005 / Revised: 19 April 2005 / Accepted: 11 May 2005 / Published online: 15 July 2005

Abstract Self-assembled monolayers (SAMs) of thiols with carboxylic acid terminal groups were formed on gold substrates. The electron transfer characteristics of redox species on the above SAM-modified electrodes were studied in acid and neutral media with the help of voltammetry under two different conditions: (1) solution phase electron transfer and (2) bridge mediated electron transfer. Two redox systems, viz., $[Fe(CN)_6]^{4-/3-}$ and $Ru[(NH_3)_6]^{2+/3+}$ were chosen for the solution phase study. Investigations of bridge mediated electron transfer were carried out by functionalising the SAM with redox moieties and then studying their redox behaviour. For this study, ferrocene carboxylic acid and 1,4-diamino anthraquinone were used and they were linked to carboxylic acid terminated thiols by covalent linkage. The voltammetric results with mercaptoundecanoic acid SAM demonstrate the difference in behaviour between *solution phase* and *bridge mediated* electron transfer processes.

Keywords Self-assembled monolayers (SAM) · Functionalised thiols · Redox systems · Electron transfer kinetics · Electron tunnelling

Introduction

Substantial research efforts are being directed towards the miniaturisation of devices to nanoscale dimensions [1–4]. Construction of nanoscale devices involves the chemical modification of surfaces with functionalised monolayers achieved through different routes such as self-assembly, electrostatic interactions, covalent linkage etc [5]. One of the popular surface derivatisation procedure is the molecular self-assembly because of its simplicity, versatility and establishment of high level order on a molecular scale [6]. Functionalisation of self-assembled monolayers (SAM) on electrode surfaces has yielded molecular assemblies exhibiting diode like electron transfer [7, 8] and interfaces showing sensing [9, 10] and catalytic [11] characteristics. Other applications include electron transfer kinetics [12–17], lithography [18] and electronic devices [19, 20]. The formation of highly ordered monolayers is often accomplished by the spontaneous adsorption of *n*-alkane thiols, *n*-alkyl silanes or their derivatives to the metal or metal oxide surfaces. Molecular layers formed by the self-assembly method are invariably more stable than those formed by the Langmuir-Blodgett (LB) method because the interaction between the adsorbed molecules and the substrate is chemisorption in the former unlike physisorption in the latter. The study of electron transfer (ET) kinetics across such monolayers is of considerable importance as follows. The study of ET blocking properties in monolayers and mixed monolayers will help us to build pore free impervious monolayers, which is an essential prerequisite to develop diode-like interfaces. The study of bridge mediated ET will lead to design of thin film sensors and catalysts. Layer-by-layer assembly of redox species/thiol or metal/thiols will lead to formation of super lattice and wire like structures [21, 22] (S. Berchmans et al, unpublished results). In this communication, investigations of ET kinetics across SAM with carboxylic acid terminal groups and their functionalised units with redox species have been undertaken. Carboxylic acid terminated thiols are particularly chosen for our investigations as they offer the possibility of further functionalisation with redox species, enzymes, catalysts etc. The ET mediated by the SAM molecular bridges with the redox species in solution and redox molecules covalently linked to these bridges are

S. Berchmans · R. G. Nirmal · G. Prabaharan
V. Yegnaraman (✉)
Central Electrochemical Research Institute,
Karaikudi 630006, India
E-mail: vyegna@rediffmail.com
Tel.: +91-4565-226204
Fax: +91-4565-227779

A. K. Mishra
Institute of Mathematical Sciences, Chennai 600113, India

investigated in detail. Earlier reports [23–25] describe the ET behaviour of SAM modified electrodes in which, the anchor-thiol molecule is initially linked to a redox moiety by a separate synthesis and then it is allowed to self- assemble on the electrode surface. Presently, a few reports [26–28] are available where a base SAM layer with functionalisable terminal groups are modified further with redox molecules such as $[Ru(NH_3)_5(4\text{-aminomethyl pyridine})](PF_6)_3$, ferrocene$[Os(bpy)_2(4\text{-aminomethyl pyridine})](Cl)(PF_6)$. In the present work, carboxyl terminated thiol is first allowed to form SAM, which is then tethered to redox species through covalent linkages using carbodiimide reagent. The structurally simple and functionalisable redox species, ferrocene carboxylic acid and 1,4-diamino-anthraquinone tethered by carbodiimide linkage are investigated in this work for the first time. This approach besides being simple will also enable the formation of a compact and ordered SAM. Moreover, the redox species and their linking strategy employed in this investigation are studied in detail for the first time. Also, the efficacy of the carboxyl terminated thiol SAMs in blocking the ET with redox species in solution has been studied. Scheme 1 depicts the two types of ET investigated in this study. The carboxylic acids chosen for investigation are represented in Scheme 2. Solution phase redox kinetics was investigated with the help of two standard redox species $[Fe(CN)_6]^{4-/3-}$ and $[Ru(NH_3)_6]^{2+/3+}$ using cyclic voltammetry. Bridge mediated ET is investigated using ferrocene carboxylic acid and 1,4-diaminoanthraquinone covalently tethered to SAMs using carbodiimide linking procedure [5].

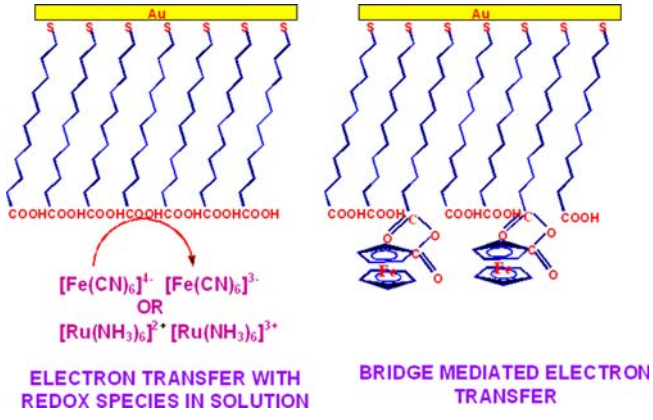

Scheme 1

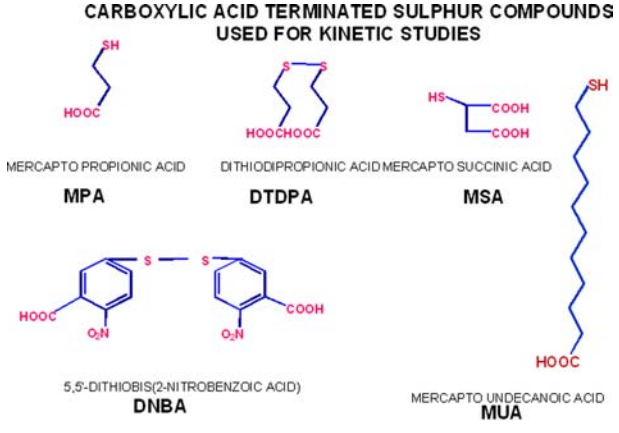

Scheme 2

Materials and methods

Reagents

The following chemicals were used as received, without further purification.

3-Mercaptopropionic acid (Merck) (MPA)
11-Mercaptoundecanoic acid 95% (Aldrich) (MUA)
3,3′-Dithiodipropionic acid 99% (Aldrich) (DTDPA)
5,5′-Dithiobis(2-nitrobenzoic acid) (DNBA)
Mercaptosuccinic acid (Merck) (MSA)
Absolute ethanol (Merck)
Sodium sulphate, GR (Merck)
Sulphuric acid, 98% (Merck)
Hexamine ruthenium (II) chloride 99.9 + % (Aldrich)
1-Cyclohexyl-3-(2-morpholinoethyl)carbodiimide metho-p-toluene sulphonate (Sigma)
Ferrocenecarboxylic acid, 97% (Aldrich) (FCA)
1,4-Diaminoanthraquinone (Sigma-Aldrich) (DAAQ)

Apparatus

The cyclic voltammetric experiments were carried out using Wenking LB75L potentiostat, Wenking (Model VSG 72) Voltage Scan Generator and a Rikadenki X-Y/t recorder and PGSTAT (Autolab).

Electrodes

Gold electrodes of area 0.07 cm^2 were used as the working electrode. Platinum foil and mercury/mercurous sulphate were used as the counter and reference electrodes respectively. Potential values mentioned in this paper are against this reference electrode. Voltammetric investigations were carried out in H_2SO_4 and Na_2SO_4 medium. 0.05 M potassium ferrocyanide and 0.0125 M ruthenium hexamine(II) chloride are used as stock solutions. All the solutions were prepared using triply distilled water.

Standardisation of gold electrodes

The gold electrodes were polished using emery papers of grade 3, 4 and 5, and then cleaned in triple distilled water followed by sonication in triple distilled water for 3 min. The cleaned electrodes were subjected to electrochemical cycling in the potential range −0.4 V to

+1.2 V. The cycling was continued till a reproducible voltammogram showing the presence of gold oxide formation and reduction was obtained. Then the electrodes were further standardised using the redox species $[Fe(CN)_6]^{4-/3-}$ in 1 M H_2SO_4 in the potential range −0.4 V to +0.4 V. The ΔE_p was measured and confirmed to be reversible. The above-standardised electrode was washed with triply distilled water followed by alcohol and acetone and air-dried. Then the electrodes are immersed in saturated solutions of respective thiols prepared in ethanol for 24 h to get SAMs on gold electrode surfaces and used for solution phase electron transfer kinetic studies.

Modification of Au electrode surfaces for bridge mediated electron transfer

Modification with ferrocene carboxylic acid

Standardised gold electrodes as treated above were immersed for 24 h in saturated ethanol solutions of respective carboxylic acid terminated thiols. The electrodes were then washed in ethanol and immersed in a solution of 0.02 M carbodiimide [prepared in phthalate buffer (pH ∽4.5)] for 1 h and washed with triply distilled water followed by immersion in FCA solution (prepared in ethanol) for 1.5 h. Finally, the electrode was thoroughly rinsed in ethanol. The modified electrode was characterised by voltammetry.

Modification with 1,4-diaminoanthraquinone

Standardised gold electrodes were immersed in saturated ethanol solutions of respective carboxylic acid terminated thiols for 24 h. The electrodes were then washed in ethanol and immersed in a solution of 0.02 M carbodiimide [prepared in phthalate buffer (pH ∽4.5)] for 1.5 h and washed with triply distilled water followed by immersion in ethanol solution of DAAQ for 3.5 h. Finally, the electrode was thoroughly rinsed in ethanol and the modified electrode was characterised by voltammetry.

Results and discussion

Solution phase ET kinetics

With $[Ru(NH_3)_6]^{2+}$

Electron transfer kinetics has been investigated at two different pH, viz., in acid medium and neutral medium using H_2SO_4 and Na_2SO_4 as the supporting electrolyte. The ET behaviour of 2 mM $[Ru(NH_3)_6]^{2+}$ in solution on Au|SAM electrodes was studied. The voltammetric data and ET rate constants obtained on Au with SAMs of MSA, MPA, DTDPA and DNBA are presented in Table 1. The typical cyclic voltammograms obtained for the SAMs of DTDPA, DNBA and MUA are given in Fig. 1a–h. The figures and the tables show that the reversible electron transfer kinetics observed in the case of $[Ru(NH_3)_6]^{2+}$ on a bare electrode decreases in the presence of SAM, which is indicated by the increase in peak separation and decrease in peak currents. The blocking of ET kinetics is found to increase with increase in chain length and ET is completely blocked in the case of MUA.

With $[Fe(CN)_6]^{4-}$

ET kinetics has been investigated at two different pH, viz., in acid medium and neutral medium using H_2SO_4 and Na_2SO_4 as the supporting electrolyte. The voltammetric behaviour of 5 mM ferrocyanide in solution on Au electrode modified with SAMs of MSA, MPA, DTDPA, DNBA and MUA has been studied. The typical cyclic voltammograms obtained in the case of DTDPA, DNBA and MUA are given in Fig. 2a–h. The results clearly indicate that the blocking of ET kinetics,

Table 1 Cyclic voltammetric data for the redox behaviour of $[Ru(NH_3)_6]^{2+/3+}$ (2.0 mM) on SAM modified electrodes

Electrode	Scan rate mV/s	Na_2SO_4 medium				H_2SO_4 medium			
		ΔE_p mV	I_{pa} μA	I_{pc} μA	k_s cm/s x 10^3	ΔE_p mV	I_{pa} μA	I_{pc} μA	k_s cm/s×10^3
Bare Au	50	75	4.1	4.1	10.5	70	7.5	7.5	14.2
	20	70	2.7	2.7	9.3	70	5.0	5.0	9.3
	10	70	2.5	2.5	6.5	70	3.5	3.5	6.5
Au|DTDPA	50	103	5.8	4.2	3.8	105	6.5	7.5	3.0
	20	100	4.0	6.5	2.6	100	4.5	5.5	2.5
	10	96	2.9	2.9	1.9	90	3.5	3.5	2.1
Au|MSA	50	100	6.9	8.5	4.0	98	3.8	8.8	4.1
	20	90	4.5	5.4	3.0	95	2.5	4.2	2.7
	10	90	3.5	3.2	2.2	92	2.0	2.6	2.1
Au|MPA	50	100	5.9	6.5	4.1	100	5.2	7.0	4.1
	20	83	3.9	4.6	4.7	89	6.5	6.3	3.0
	10	83	3.0	3.8	3.9	81	5.0	4.5	3.4
Au|DNBA	50	102	5.5	6.5	3.5	78	3.3	4.4	8.7
	20	110	4.2	5.0	1.7	78	2.3	3.8	5.5
	10	96	2.7	3.6	1.7	78	2.1	2.8	4.6

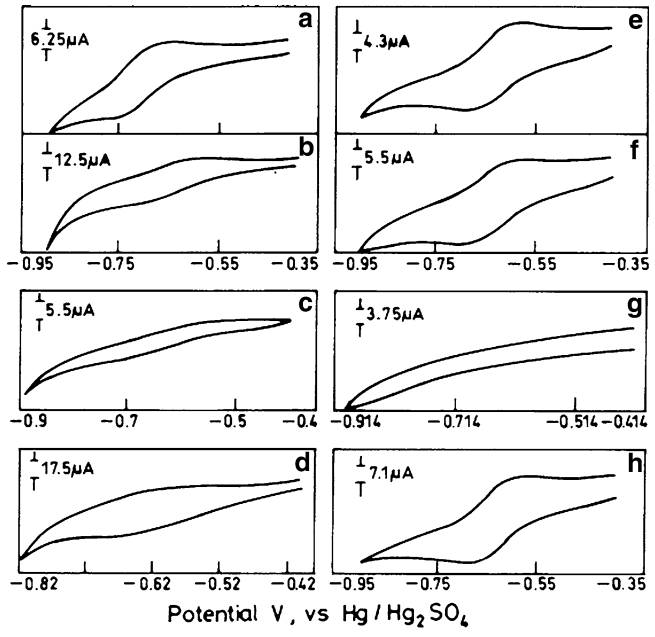

Fig. 1 Cyclic voltammograms representing the response for 2.0 mM ruthenium hexamine in H_2SO_4 on **a** bare Au, **b** Au|DTDPA, **c** Au|MUA and **d** Au|DNBA electrodes. Scan rate = 50 mV/s. Cyclic voltammograms representing the response for 2.0 mM ruthenium hexamine in Na_2SO_4 on **e** bare Au, **f** Au|DTDPA **g** Au|MUA and **h** Au|DNBA. Scan rate = 50 mV/s

is found to increase with increase in chain length and ET is completely blocked, in the case of mercaptoundecanoic acid with 11 carbon atoms. In the case of shorter chain thiols ET is made slower due to the presence of the monolayer, which is revealed by increase in peak separation between the anodic and cathodic peaks.

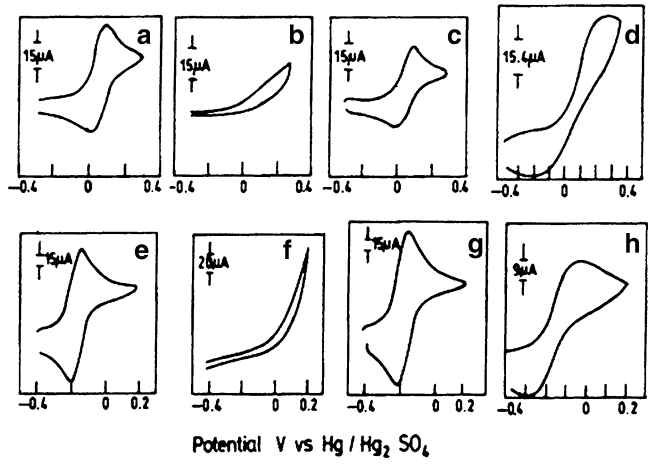

Fig. 2 Cyclic voltammograms representing the response for 5.0 mM ferro cyanide in H_2SO_4 on bare Au **b** Au|MUA, **c** Au|DTDPA and **d** Au|DNBA electrodes. Scan rate = 50 mV/s. Cyclic voltammograms representing the response for 5.0 mM ferrocyanide in Na_2SO_4on **e** bare Au, **f** Au|MUA, **g** Au|DTDPA and **h** Au|DNBA electrodes. Scan rate = 50 mV/s

Discussion

The ET kinetics across a carboxylic acid terminated thiol SAM is determined by electrostatic interactions, thiol chain length and structural organisation. The pk_a values of carboxylic acid terminated thiols used in this investigation lie in the range 3.0–5.5.

Electrostatic interactions

The pKa values indicate that the –COOH terminal groups will attain negative charge at neutral pH. This will have a discriminating influence between the electron transfer kinetics of a positively charged ruthenium hexamine species and a negatively charged ferrocyanide anions. It can be seen from Figs. 1 and 2, that in the case of ruthenium hexamine cations the influence of electrostatic interactions is clearly noticed. The electron transfer is facilitated at neutral pH when the SAM layer and the electroactive species are oppositely charged. In the case of ferrocyanide anions, the electron transfer rate is expected to decrease as the SAM layer and the ferrocyanide anions are of the same charge. However, ferrocyanide anions are known to bind with the cations of the electrolyte and form a bridge, which helps to overcome the influence of electrostatic interactions and contribute to an increase in electron transfer kinetics. Hence there is not much change in the electron transfer kinetics after the formation of SAMs in the case of short chain thiols. However, the electron transfer is completely blocked in the case of MUA due to structural organisation and chain length as discussed below.

Length of the carbon chain

The carbon chain length in thiol molecule also determines the ET kinetics. As the distance between the electrode surface and the redox species is altered by the spacer molecules (thiol molecules in this case), the ET kinetics decreases as described by the Marcus equation.

$$I = I_0 e^{-\beta d},$$

where I and I_0 are the currents on Au|SAM and Au electrodes respectively, d is the thickness of the SAM and β is a constant. It can be seen clearly in the case of MUA with 11 carbon atoms where ET is almost completely blocked. However, in the case of DNBA (a molecule with the spacer length of a benzene molecule) the ET occurs with less reversible or slow kinetics. In the case of shorter molecules like MSA and DTDPA, nearly reversible response with a decreased peak current is observed.

Structural organisation

Generally, there are two kinds of defects in a thiol monolayer: pinhole and collapsed site defects. A pinhole

is a site at which the electrode surface is exposed to the electrolyte. Molecules and ions from the electrolyte can reach the electrode surface through pinholes. A defect is a site at which molecules and ions from the electrolyte can approach the electrode surface at a distance shorter than the thickness of the SAM. Therefore, the ET in SAMs is controlled by the electron transfer at pinholes, at collapsed sites and at defect free domains.

Sabatani and Rubinstein [30] and Finklea et al. [31] demonstrate that the pinholes in thiol monolayers could be regarded as microarray electrodes. The model of microarray electrode proposed by Amatore et al. [32] assumes that pinholes are disk shaped active regions with uniform radius and are evenly distributed in SAM. The schematic representation of the pinholes is given in Scheme 3. If the pinholes formed in the monolayer are very small and widely separated relative to the diffusion layer thickness, sigmoidal shaped voltammograms will be obtained showing the characteristics of a nanoelectrode ensemble at which the radial diffusion layer developed at individual nanoelectrodes

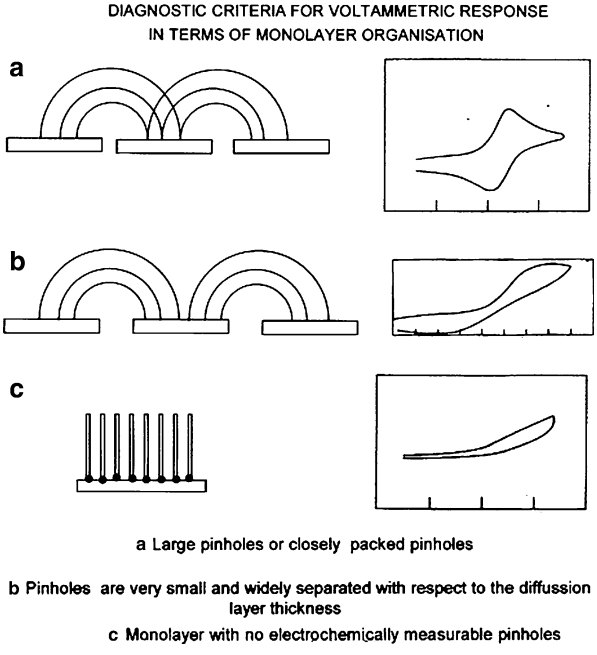

Scheme 3

are isolated from each other. Large pinholes or closely packed small pinholes will result in peak shaped voltammograms similar to those observed on a macroelectrode. In the case of long chain alkane thiols, the monolayers are highly ordered and are devoid of electrochemically measurable pinholes. The electron transfer rate at defect free domains will be less than the electron transfer rate at defects (including pinholes and collapsed sites). In the case of defect free domains electron tunnelling takes place.

The above discussions reflect that peak shaped voltammograms obtained in most of the cases discussed in this work show that we are dealing with situations of large pinholes or closely packed small pinholes, which have given rise to peak shaped voltammograms, similar to the case of macroscopic electrode. In the case of MUA complete blocking of ET kinetics is observed. This shows that the SAM is devoid of electrochemically measurable pinholes and consists of defect free domains. In this case tunnelling of electrons takes place and according to Marcus equation ($\ln I = \ln I_o - \beta d$) the tunnelling currents are expected to decrease exponentially with monolayer thickness. Hence very low currents are observed in the case of MUA. In the case of DNBA sigmoidal behaviour is observed which corresponds to an ultra microelectrode behaviour.

Bridge mediated ET kinetics

The redox species, viz., DAAQ and FCA, have been presently chosen for studying the bridge mediated electron transfer kinetics. Both the molecules are known to exhibit reversible ET kinetics at the electrode/electrolyte interface and are tethered to carboxylic acid terminated thiols through covalent linkage with the formation of an anhydride bond in the case of FCA [7] and an amide bond in the case of DAAQ. The modified electrodes are characterised by voltammetry and the voltammetric data are presented in Tables 2–4.

The voltammetric data obtained for the redox characteristics of FCA linked to Au|DTDPA, Au|MSA and Au|MUA electrodes are given in Table 2. Typical voltammograms depicting the redox behaviour of FCA linked to Au|MSA and Au|DTDPA electrodes are

Table 2 Voltammetric data for the bridge mediated system: FCA linked through covalent linkage; Na_2SO_4 medium

Sl. no.	Surface	Scan rate mV/s	ΔE_p mV	K_s s^{-1}	E_o mV	E_{FWHM} mV	i_{pa} μA	i_{pc} μA	i_{pa}/v $\mu F/cm^2 \times 10^4$	Coverage (Ox) $mol/cm^2 \times 10^{-10}$	Coverage (Red) $mol/cm^2 \times 10^{-10}$
1.	Au|DTDPA|FCA	500	30	21.28	−185	240	24.75	10.5	0.5	16.50	4.93
		400	30	17.02	−175	180	11.25	4.50	0.3	14.80	1.81
		300	30	12.76	−165	150	9.75	4.50	0.3	6.60	1.99
2.	Au|MSA|FCA	500	75	7.23	−290	370	10.50	9.75	0.2	9.20	6.14
		400	72.5	5.78	−275	350	9.75	9.00	0.2	10.00	6.10
		300	70	4.78	−270	330	9.00	6.75	0.2	11.97	6.89
3.	Au|MUA|FCA	500	80	6.60	−255	190	2.00	0.75	0.04	0.88	0.18
		400	80	5.28	−246	180	1.75	0.50	0.04	0.88	0.18
		300	80	3.96	−242	170	1.45	0.40	0.04	0.90	0.14

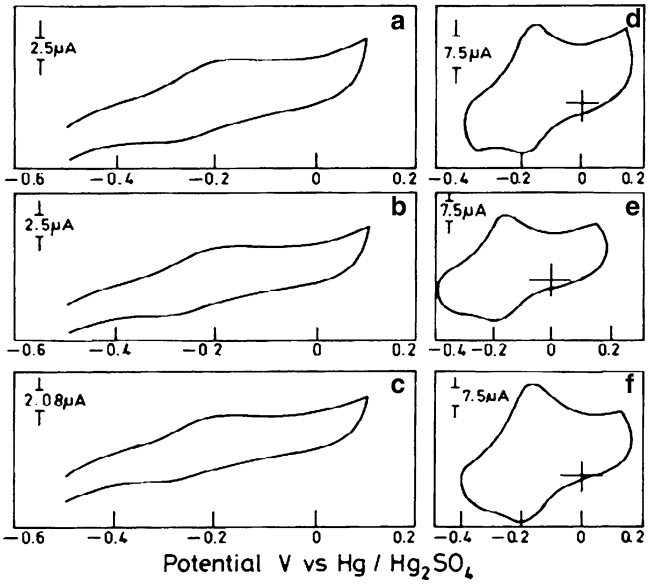

Fig. 3 Cyclic voltammograms representing the response in Na_2SO_4 for **a** Au|MSA|FCA; scan rate = 500 mV/s **b** Au|MSA|FCA; scan rate = 400 mV/s **c** Au|MSA|FCA; scan rate = 300 mV/s **d** Au|DTDPA|FCA; scan rate = 300 mV/s **e** Au|DTDPA|FCA; scan rate = 400 mV/s **f** Au|DTDPA|FCA; scan rate = 500 mV/s

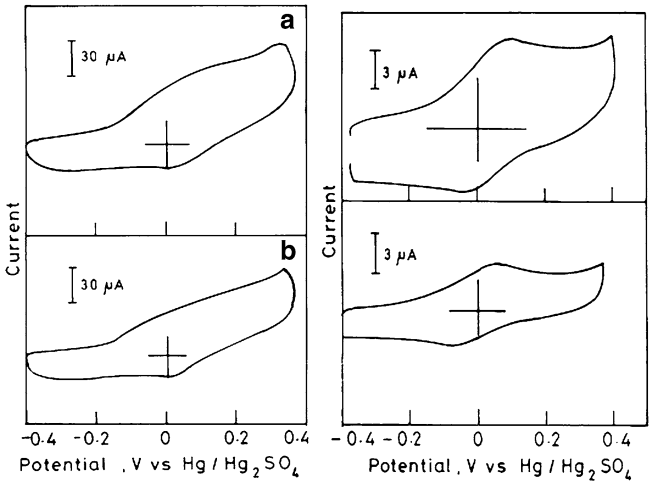

Fig. 4 Cyclic voltammograms representing the response in H_2SO_4 for **a** Au|MPA|FCA ; scan rate = 300 mV/s **b** Au|MPA|FCA; scan rate = 200 mV/s **c** Au|DTDPA|FCA; scan rate = 50 mV/s **d** Au|DTDPA|FCA; scan rate = 20 mV/s

presented in Fig. 3a–f. Estimation of coverage, carried out using the integration of peak area, reveals that it corresponds to a monolayer. E_{FWHM} values are high in all the three cases, especially very high in the case of MSA. They are greater than the theoretically expected value of 90.6/n in all the cases. The rate constants vary in the following order

DTDPA > MSA > MUA

In the case of DTDPA SAM, the ΔE_p value observed is less compared to MSA and MUA and is expected to have a higher rate constant. However, in all the cases the surface coverage corresponding to oxidation is higher than that due to reduction suggesting some kinetic limitation during the reverse process. The ratio of i_p with scan rate is found to be constant indicating the surface nature of the process. The coverages have been estimated using the integration of peak area and ET rate constant for the surface modified species has been calculated using the method of Laviron [33].

By using the expressions for current from surface voltammetry, Laviron [33] has evolved conditions for the determination of rate constants (k_s) from the experimental quantity, ΔE_p, the difference between the anodic and cathodic peak potentials. The variation of $n(E_p - E_{0'})$ as a function of 1/m is followed, where $m = (RT/F)(k_s/nv)$. When $\Delta E_p > 200/n$ mV, α and k_s can be obtained experimentally by plotting E_p as a function of log v, which yields straight line plots with a slope equal to $-2.3RT/\alpha nF$ for the cathodic peak and 2.3 $RT(1-\alpha)nF$ for the anodic. k_s can be calculated using the following equation

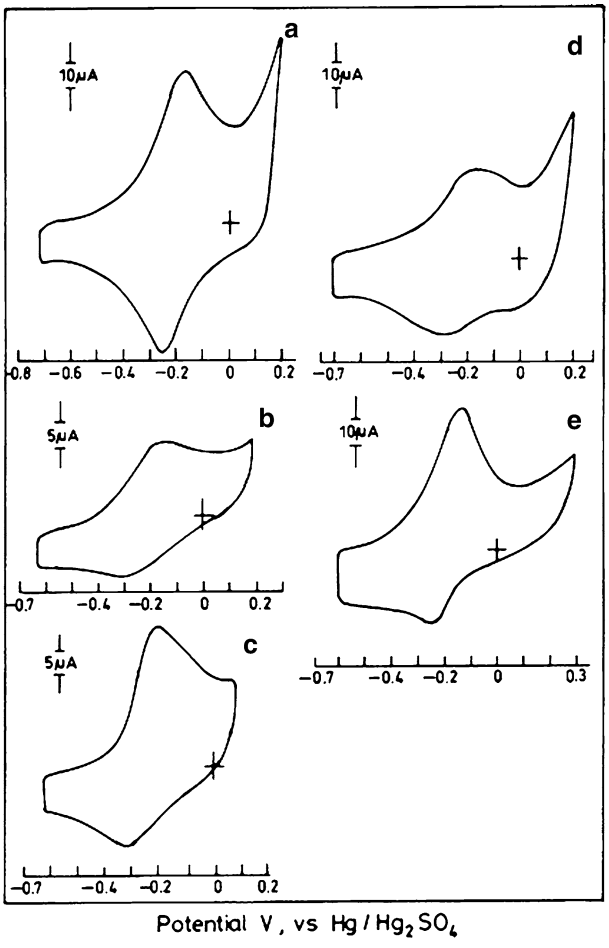

Fig. 5 Cyclic voltammograms representing the response for **a** Au|MSA|DAAQ in H_2SO_4, **b** Au|MUA|DAAQ in H_2SO_4 **c** Au|MUA|DAAQ in Na_2SO_4, **d** Au|MSA|DAAQ in Na_2SO_4, **e** Au|DTDPA|DAAQ in Na_2SO_4; scan rate = 800 mV/s

$$\log k = \alpha \log(1-\alpha) + (1-\alpha) - \log(RT/nFv) - \alpha(1-\alpha)nF\Delta E_P/2.3RT,$$

which is valid for $\Delta E_p > 200/n$ mV.

The electrochemical response of FCA modified electrode is not very well defined in some SAMs in H_2SO_4 medium. In the case of MPA, the anodic current starts rising around the E_o' value of FCA which affects the response of FCA (Fig. 4a, b). In the case of DTDPA, well defined response is obtained in sulphuric acid medium even at low scan rates (Fig. 4c, d). Generally in the voltammograms of all the cases, the surface coverage corresponding to oxidation is higher than that due to reduction suggesting some kinetic limitation during the reverse process. The effect of anions in the supporting electrolyte with the surface-immobilised ferrocenium ions has been reported earlier [34] and it is observed that the ion pairs formed between the anions of the supporting electrolyte and the ferricinium cations stabilise the system. The reason is due to the stability of ion pairs formed between the anions of the supporting electrolyte and the ferricinium ions. Hence reduction tends to become difficult. The electrochemical reduction is possibly preceded by the chemical step of dissociation of ion pairs, following an EC mechanism as follows.

$$\begin{aligned} Fc - e &\longrightarrow Fc^+ \\ Fc^+ + HSO_4 &\rightleftharpoons \left(FC^+\right)\left(HSO_4^-\right) \\ Fc^+ + e &\longrightarrow Fc \end{aligned}$$

This could possibly explain the observed cathodic peak coverage being relatively smaller than the anodic peak coverage.

In the case of DAAQ, reversible peaks are obtained in both Na_2SO_4 and H_2SO_4 (Fig. 5a–e and Tables 3 and 4). Better reversibility is observed in H_2SO_4 medium compared to Na_2SO_4 medium as revealed by lower ΔE_p values in the case of Au/MSA. E_{FWHM} values are smaller in the case of H_2SO_4 than in Na_2SO_4 in the case of MSA. In the case of MUA similar values are obtained in both acidic and neutral media. The surface coverage for oxidation and reduction processes is of the same order in the case of MUA. This suggests that the DAAQ molecules are favourably linked to the monolayer in a proper orientation compared to FCA molecules. The favourable orientation has led to facile kinetics and hence oxidation and reduction processes occur to the same extent in these cases. E_0' values are found to be almost constant with respect to scan rate. The most sensitive criterion for rapid kinetics in the ET reaction is that $\Delta E_p = 0$ at any scan rate. And non-zero, potential scan rate dependent ΔE_p is expected if ET is slow. The wave shape also changes. Scan rate dependent ΔE_p for the immobilised species is interpreted in terms of slow ET kinetics. Usually experimentally reported E_{FWHM} values vary over a range from 100 mV to 300 mV. Explanations which have been offered for the general broadening of voltammetric peaks are: (1) in an ensemble of attached species, slight variation in surface structure during solvation causes a narrow spectrum of E_0' surface values rather than one unique value [5].

Table 3 Voltammetric data for the bridge mediated system: DAAQ linked through covalent linkage; Na_2SO_4 medium

Sl. no.	Surface	Scan rate mV/s	ΔE_p mV	K_s s^{-1}	E_o^1 mV	E_{FWHM} mV	i_{pa} μA	i_{pc} μA	i_{pa}/v AsV^{-1} $\times 10^4$	Surface coverage (Ox) $mol/cm^2 \times 10^{-10}$	Surface coverage (Red) $mol/cm^2 \times 10^{-10}$
1.	Au|DTDPA|DAAQ	800	120	3.1	−205	200	40	15	0.5	6.6	2.1
		400	100	2.3	−205	200	16	07	0.4	5.3	1.6
		200	90	1.4	−200	200	07	02	0.4	6.9	2.4
2.	Au|MSA|DAAQ	800	120	3.1	−240	250	15	13	0.18	4.1	2.9
		400	110	1.8	−240	250	06	06	0.15	3.2	2.8
		200	110	1.1	−240	250	2.4	2.4	0.12	2.0	1.7
3.	Au|MUA|DAAQ	800	120	3.1	−255	250	18.5	11	0.23	2.9	2.9
		400	110	1.8	−255	250	6.5	04	0.16	2.2	2.2
		200	110	1.1	−255	250	02	02	0.10	2.6	2.2

Table 4 Voltammetric data for the bridge mediated system: DAAQ linked through covalent linkage; H_2SO_4 medium

Sl. no.	Surface	Scan rate mV/s	ΔE_p mV	K_s s^{-1}	E_o^1 mV	E_{FWHM} mV	i_{pa} μA	i_{pc} μA	i_{pa}/v $AsV^{-1} \times 10^4$	Surface coverage (Ox) $mol/cm^2 \times 10^{10}$	Surface coverage (Red) $mol/cm^2 \times 10^{10}$
1.	Au|MSA|DAAQ	800	80	7.0	−215	190	36	36	0.45	6.7	6.7
		400	70	4.5	−210	190	18	18	0.45	7.0	5.7
		200	70	2.3	−205	190	08	08	0.40	5.6	5.3
2.	Au|MUA|DAAQ	800	130	2.5	−235	240	8.5	06	0.10	1.9	1.9
		400	130	1.2	−250	240	05	03	0.12	2.2	2.2
		200	130	0.6	−250	240	03	02	0.13	2.4	2.2

Surface activity coefficients vary with coverages$\lceil_0$ and$\lceil_R$.]] > (2)Anson [35] proposed 'interaction parameters' that are responsible for narrowing down or broadening of peaks. Broadening of peak ($E_{FWHM} > 90.6$/n) is referred to having surface immobilised species with repulsive or destabilising interactions and narrowing down of peak ($E_{\mathrm{FWHM}} < 90.6$/n) is due to attractive interactions between the species.

Both redox-modified electrodes, in the present studies, exhibit $E_{\mathrm{FWHM}} > 90.6$/n. Hence the situation corresponds to that of destabilizing/repulsive interactions. Non-zero ΔE_{p} corresponds to relative lowering of ET kinetics. The i_{p}/v values for both the cases remained constant indicating the 'surface-confined' nature of the species. The reactivity varies as DTDPA > MSA > MUA for FCA modification. For the DAAQ modified electrodes in Na_2SO_4, the ET rate constants have almost similar values for the three SAMs used as anchor. However, in H_2SO_4 medium, the rate constant vary as MSA > MUA.

This work differentiates between the two types of ET observed in the case of redox species present in solution and redox species tethered to the thiol chains through –COOH terminal groups. The ET mechanism observed in the case of redox species present in solution is summarised in Scheme 3. The results confirm that increase in chain length increases the ET blocking properties and in the case of MUA, which is devoid of electrochemically measurable pinholes, the ET can occur only through tunnelling (Figs. 1b, f; 2c, g). In the case of bridge mediated electron transfer, the redox response of FCA and DAAQ could be observed on Au|SAM electrodes linked to redox species (Figs. 3–5]. This suggests that when the redox species is tethered to the alkane thiol chain, the electron conductivity occurs through the bonds, whereas in the case redox species in solution the electron conductivity/tunnelling can occur only through space. However, it requires further detailed investigations to understand the ET mechanism.

Conclusions

A detailed analysis of the electron transfer kinetics has been carried out in the solution phase using standard redox species and as bridge mediated systems with the redox species tethered to the carboxylate functional groups of thiols acting as anchors. The difference in electron transfer kinetics observed in the case of solution phase electron transfer and bridge mediated electron transfer is clearly demonstrated in the case of Au|MUA electrode. The results present the scope of using the carboxylic acid terminated thiols for further functionalisation leading to different applications and analysing the characteristics of the SAM modified electrodes using solution phase electron transfer kinetics. The utility of bridge mediated systems for applications such as fabrication of diode like interfaces and as sensing platforms for glucose and sucrose has already been reported by us.

Acknowledgements The DRDO, New Delhi is gratefully acknowledged for financial support.

References

1. Willner I, Willner B (1997) Adv Mater 9:51
2. Willner I, Willner B (1998) J Mater Chem 8:2543
3. Drexler KE (ed) (1992) Nanosystems-molecular machinery, manufacturing and computation. Wiley, New York
4. Patolsky F, Gabriel T, Willner I (1999) J Electroanal Chem 479:69
5. Murray RW (1984) In Bard AJ (ed) Electroanalytical chemistry, vol 13, Chapter 3. Marcel Dekker, New York
6. Finklea HO (1996) In Bard AJ, Rubinstein I (eds) Electroanalytical chemistry, vol 19. Marcel Dekker, New York, pp 109–335
7. Berchmans S, Ramalechume C, Lakshmi V, Yegnaraman V (2002) J Mater Chem 12:2538
8. Gittins DI, Bethell D, Nichols J, Schiffrin DJ (2000) J Mater Chem 10:79
9. Berchmans S, Sathyajith R, Yegnaraman V (2002) Mater Chem Phys 77:390
10. Swaminatha Prabu K, Berchmans S, Yegnaraman V (2000) Abs No 966, The 198th meeting of the electrochem. Soc, Phoenix, October 22–27
11. Berchmans S, Yegnaraman V, Sandhyarani N, Murty KVGK, Pradeep T (1999) J Electroanal Chem 170:468
12. Berchmans S, Yegnaraman V, Prabhakara Rao G (1998) J Solid State Electrochem 3:52
13. Berchmans S, Yegnaraman V, Prabhakara Rao G (1997) Proc Indian Acad Sci (Chem Sci) 109(4):277
14. Younan Xia, John A Rogers, Kateri E. Paul, George M Whitesides (1999) Chem Rev 99:1823
15. Jon Hendrik Schon, Hong Meng, Zhenan Bao (2001) Nature 413:713
16. Aviram A, Ratner MA (1974) Chem Phys Lett 29:277
17. Clegg RS, Hutchison JE (1999) J Am Chem Soc 121:5319
18. Che G, Li Z, Zhang H, Cabrera CR (1998) J Electroanal Chem 453:9
19. Yang D, Zi M, Chen B, Gao Z (1999) J Electroanal Chem 470:114
20. Diao P, GuO M, Jiang D, Jia Z, Cui X, Gu D, Tong R, Zhong B (2000) J Electroanal Chem 480:59
21. Sarathy KV, Thomas PJ, Kulkarni GU, Rao CNR (1999) J Phys Chem B 103:499
22. Pethkar S, Aslam M, Mulla LS, Ganeshan P, Vijayamohanan K (2001) J Mater Chem 11:1710
23 Daniel Bretts JL, Rhian Williams, Paul Wilde C (2002) J Electroanal Chem 538–539:65
24 Tender L, Carter MT, Murray RW (1994) Anal Chem 66:3173
25 Weber K, Creager SE (1994) Anal Chem 66:3164
26 Haddox RM, Finklea HO (2004) J Phys Chem B 108:1694
27 Smalley JF, Finklea HO, Chidsey CED, Linfond MR, Creager SE, Ferraris JP, Chalfant K, Zawodzinek T, Feldberg SW, Newton MD (2003) J Am Chem Soc 125:2004
28 Finklea HO, Yoon K, Chamberlain E, Allen J, Haddox R (2001) J Phys Chem B 105:3088
29 Nicholson RS, Shain I (1965) Anal Chem 37:1351
30 Sabatani E, Rubinstein I (1987) J Phys Chem 91:6663
31 Finklea HO, Srider DA, Fedyk J, Sabatani E, Gafni Y, Rubinstein I (1993) Langmuir 9:3660
32 Amatore C, Saveant JM, Tessier D (1983) J Electroanal Chem 147:39
33 Laviron E (1979) J Electroanal Chem 101:19
34 Bard AJ, Rubinstein I (1996) Electroanalytical chemistry. Marcel Dekkar Inc. Vol. 19, p255
35 Brown AP, Anson FC (1977) Anal Chem 49:1587